Solar Energy Materials & Solar Cells 95 (2011) 721–726

Contents lists available at ScienceDirect

Solar Energy Materials & Solar Cells

journal homepage: www.elsevier.com/locate/solmat

Effect of gallium grading in Cu(In,Ga)Se_2 solar-cell absorbers produced by multi-stage coevaporation

Sebastian Schleussner [a,*], Uwe Zimmermann [a], Timo Wätjen [a,b], Klaus Leifer [b], Marika Edoff [a]

[a] Solid State Electronics, Uppsala University, P.O. Box 534, SE-751 21 Uppsala, Sweden
[b] Electron Microscopy and Nanoengineering, Uppsala University, P.O. Box 534, SE-751 21 Uppsala, Sweden

ARTICLE INFO

Article history:
Received 17 December 2009
Received in revised form
9 September 2010
Accepted 15 October 2010
Available online 30 October 2010

Keywords:
CIGS
Coevaporation
Multi-stage process
Three-stage process
Gradients

ABSTRACT

We investigate Cu(In,Ga)Se_2 thin films grown in multi-stage coevaporation processes and solar cells fabricated from such absorbers. Despite some interdiffusion during film growth, Ga/(Ga+In) gradients defined via evaporation-profile variations in the process are to a good part retained in the finished film. This indicates that the bandgap can be engineered in this type of process by varying the evaporation profiles, and consequently also that unintended profile variations should be noted and avoided. With front-side gradients the topmost part of many grains seems to be affected by a higher density of lattice defects due to the strong change of gallium content under copper-poor growth conditions. Electrically, both back-side gradients and moderate front-side gradients are shown to yield an improvement of device efficiency. If a front-side gradient is too wide, though, it causes strong voltage-dependent collection and the fill factor is severely reduced.

1. Introduction

The latest record-efficiency solar-cell devices based on Cu(In,Ga)Se_2 (CIGS) featured absorbers prepared by three- or multi-stage evaporation processes [1,2]. This is at least in part attributed to the fact that this process gives rise to a spontaneous 'notch' grading of the gallium content $x := [Ga]/[In+Ga]$ [3], for which Gabor et al. offer a growth model [4]. By changing the gallium content from $x=0$ to 1, the bandgap of CIGS can be adjusted approximately from 1.0 to 1.7 eV, with the bandgap variation affecting almost exclusively the position of the conduction-band edge (see for instance [5]). Thus, the 'notch' structure is equivalent to a low-bandgap semiconductor layer being sandwiched between two layers of higher bandgap that was projected by modelling to be optimal for device performance [6].

As the Ga content decreases from the rear towards the middle of the absorber it induces a back-surface field in the conduction band [7,8], which causes electrons to drift away from the rear contact and thereby reduces the risk of recombination at the contact. In this way, the back-surface grading can improve the open-circuit voltage V_{OC}. It may also marginally increase the short-circuit current density J_{SC} thanks to an improvement of the carrier-collection efficiency close to the rear contact.

The potential benefit of front-surface grading as represented by the second part of the notch structure is the decoupling of photogeneration and carrier recombination [5]. As Dullweber et al. [9] have found, the optical bandgap determining J_{SC} in frontside-graded CIGS corresponds well to the minimum bandgap $E_{g,min}$, while interface recombination and thus V_{OC} depend on the bandgap in the space-charge region, $E_{g,SCR}$. At the same time, it has to be kept in mind that too wide or too strong Ga gradients may act as barriers for electrons on their way to the junction. This would cause poor and voltage-dependent photocurrent collection [10].

In this work we show that intentional Ga grading added to the spontaneous gradients is retained to a good degree in CIGS absorbers grown by multi-stage coevaporation. We also examine the influence of various gradings on the performance of solar-cell devices prepared from those absorbers and present some guidelines for the design of high-efficiency CIGS solar cells.

2. Experimental

2.1. CIGS and device fabrication

The solar-cell devices were fabricated on 1-mm thick sheets of soda-lime glass with molybdenum back contacts of 300 nm thickness deposited by DC magnetron sputtering, in accordance with our group's baseline procedure [11].

The CIGS layers were deposited by coevaporation of the elements Cu, In and Ga from fast-acting open boat sources in a Se atmosphere maintained from a crucible source kept at a constant temperature. The metal rates were controlled using mass-spectrometer feedback.

* Corresponding author. Tel.: +46 184713113; fax: +46 18555095.
E-mail address: sebastian.schleussner@angstrom.uu.se (S. Schleussner).

0927-0248/$ - see front matter © 2010 Elsevier B.V. All rights reserved.
doi:10.1016/j.solmat.2010.10.011

The Se temperature was chosen such that it was safe to assume that the Se evaporation rate was several times higher than that required for the formation of stoichiometric Cu(In, Ga)Se_2 at all times during the process. The process was carried out in a vacuum chamber pumped to a pressure of below 2×10^{-6} mbar holding three 5×5 cm^2 substrates per run. Further details on the CIGS processes are given in Section 2.3 below.

Device completion once more followed our group's baseline procedure, comprising a 50-nm CdS buffer layer grown by chemical bath deposition, an RF-sputtered 50-nm layer of intrinsic ZnO, a DC-sputtered 300-nm film of Al-doped ZnO as a conductive window layer, a current-collecting Ni–Al–Ni grid and mechanical scribing to define separated 0.5 cm^2 cells. Every processed sample comprises 16–32 individual cells.

2.2. Analyses

The composition of the CIGS films was determined by X-ray fluorescence (XRF) performed in a *Spectro X-lab 2000* and the thickness was measured with a *Dektak V 200-Si* profilometer. The XRF countrates were scaled with a linear model to yield atomic percentages. Elemental depth profiles of absorbers capped with the CdS buffer layer were analysed by means of secondary ion mass spectrometry (SIMS) in a *Cameca IMS 4f* system, using Cs^+ ions at 9 kV acceleration voltage, and detecting MCs^+ complexes (M= ^{63}Cu, ^{69}Ga, ^{80}Se, ^{98}Mo and ^{115}In).

The symbols $x \coloneqq [Ga]/[In+Ga]$ and $y \coloneqq [Cu]/[In+Ga]$ are used in the following to denote the atomic ratios of gallium versus both group-III elements and copper versus the group-III elements, respectively; in particular, x^* and y^* stand for the *final*, average gallium and copper contents as measured by XRF.

The recipe and SIMS graphs are scaled such that for every element, the average of the profile matches the corresponding content according to the XRF data. For the recipe graphs, we assume a constant sticking coefficient for each of the evaporated metals. The x-axis of the SIMS depths profiles is calibrated with the measured film thickness, assuming a constant sputter rate.

Transmission-electron microscopy (TEM) analyses were performed on several samples in a *FEI Tecnai F30 ST* microscope operating at 300 kV; also electron-micro-diffraction patterns were viewed here. Energy-dispersive X-ray analysis (EDX) line scans of the samples were recorded while in scanning transmission-electron microscope (STEM) mode. In contrast to the SIMS data, the EDX spectra were translated into composition data based on a standardless quantification only and not further calibrated with XRF results. This is the reason for the discrepancy between the two methods that is seen in Fig. 3.

Cells were characterised by current versus voltage (IV) measurements with illumination from an ELH lamp. The external quantum efficiency (QE) was determined under ambient light, using chopped monochromatic light that was scanned through the wavelength interval of 360–1200 nm in 10-nm steps.

2.3. CIGS recipe specifics

Fig. 1(a) shows the rate and temperature profiles of the reference CIGS recipe which contains no gallium grading in the evaporation profiles. Our CIGS process is based on the three-stage process [3], where the evaporation of In, Ga and Se on a relatively cool substrate ('stage *I*') is followed by the evaporation of Cu and Se at a high temperature ('stage *II*'), which after a transition of the composition to Cu-richness is capped by further evaporation of the group-III elements In and Ga together with Se ('stage *III*') to make the final film Cu-poor. Differing from the most basic three-stage processes, our recipe features an overlap of the stages *II* and

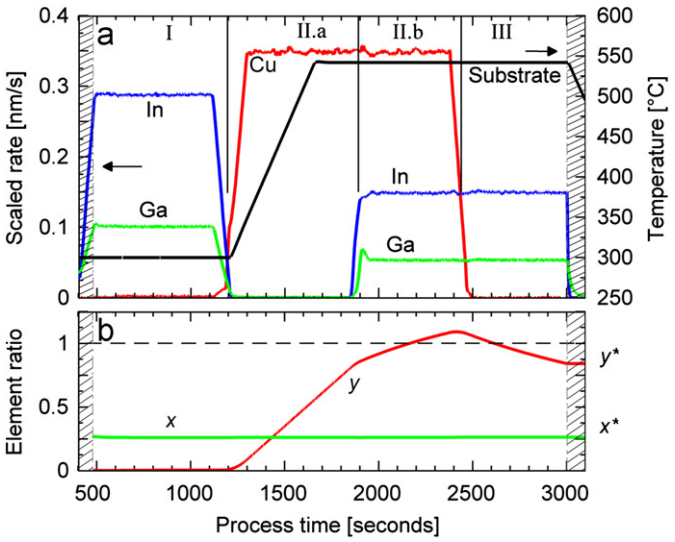

Fig. 1. (a) Evaporation rates of the metals Cu, In and Ga and substrate temperature of the ungraded reference process **A** as a function of process time. The rates are scaled data from the in situ mass spectrometer. (b) Integrated composition in terms of the ratios $x=[Ga]/[In+Ga]$ and $y=[Cu]/[In+Ga]$.

Table 1
Process parameters for the samples discussed in this paper.

Sample	Thickness (μm)	x^*	y^*	t_I (s)	t_{IIa} (s)	t_{IIb} (s)	t_{III} (s)	t_{Ia} (s)	t_{IIIb} (s)
A	1.71	0.26	0.84	720	690	570	540	–	–
B	1.63	0.28	0.85	720	690	570	540	180	–
C	1.70	0.29	0.86	720	690	570	540	180	140
D	1.58	0.32	0.89	720	690	570	540	180	300

Thickness, x^* and y^* denote the actually obtained absorber thickness and average composition. The times t_N refer to the durations of the respective stages *N*. Dashes '–' in these columns mean that the corresponding grading was not applied.

III. This emulates the configuration in an inline system, where the low-temperature stage *I* is located in its own segment of the vacuum system but stages *II* and *III* are closer together. Because of the overlap, we refer to our process as a *multi-stage* process, with the basic phases denoted as marked in Fig. 1. We divide stage *II* further into the Cu-only stage *II.a*, and stage *II.b* where both Cu and the group-III elements are evaporated. The durations of the various stages are listed in Table 1. We use box-like evaporation profiles in order to make the definition of gradings straight-forward. Another characteristic of our recipe is the relatively long third stage. This allows for a larger process window in our rate-controlled system, which does not use end-point detection [12]. The substrate was kept at a temperature of 300 °C during the first stage. During the second stage this temperature was ramped up to 540 °C and it was then held at that value until the end of the evaporation. After that, the heater was turned off and the samples left to cool in the vacuum.

Fig. 1(b) displays the development of the *integral* of the film composition in the reference process over time, as calculated from the final composition and the given evaporation profiles. These values can be thought of as estimations of the result of XRF measurements at the corresponding points in time. Note the constant level of the gallium-to-group-III ratio x for evaporation in this recipe, and how the copper-to-group-III ratio y moves to a value above unity and then back. We compare this reference recipe, which has given rise to sample **A**, with three recipes where the